# EXPERIMENTAL INVESTIGATION OF GASEOUS MIXTURES OF ETHANE, METHANE, AND $CO_2$ AS AN ALTERNATIVE TO CONVENTIONAL FUEL IN SI ENGINES

**Matthew Gore, Kaushik Nonavinakere Vinod, Tiegang Fang***

**Department of Mechanical and Aerospace Engineering, North Carolina State University, 1840 Entrepreneur Drive, Raleigh, NC 27695-7905, USA**

***Corresponding Author Email: tfang2@ncsu.edu**

## ABSTRACT

*This study investigates the viability and performance of certain synthetics fuels in spark ignition internal combustion engine based stationary power generation wherein the fuel comprises a mixture of methane and ethane in high dilutions of carbon dioxide. The fuel of concern is a byproduct of a novel method for producing ethylene from ethane. The byproduct gas mixture has a concentration of approximately 41% $CO_2$, 40% ethane, and 5% methane by weight along with other minor compounds. Varying mixtures of ethane and methane combined with between 42% to 46% by weight $CO_2$ were used to evaluate the viability and efficiency of this fuel to operate in existing internal combustion engines as a means for reducing emissions and increasing industrial process efficiency. A 13 hp gasoline generator was repurposed as a test stand by incorporating a modified fuel induction system and instrumentation for data collection. A gas metering and mixing system was installed to precisely control the mass flow of gasses induced into the engine. Various instrumentation was installed to monitor in-cylinder pressure, temperature at various locations, emissions, and fuel and airflow rates. Varying fuel mixtures and loads were tested and compared to gasoline. It was found that under a high load, the mixed gas was able to generate comparable thermal efficiency and power to gasoline. But under no load or a part load condition the indicated thermal efficiency was found to be about 21% lower than that of gasoline. Further, the mixed gas also resulted in up to 50% reduction in CO and NOx emissions when compared to gasoline.*

**Keywords**: High $CO_2$ fuel; Ethane and methane combustion; Cl-ODH byproducts; Spark-ignition engine; Power generation; EGR

## 1. INTRODUCTION

Ethylene is an important industrial organic chemical having a variety of uses in the medical, polymer, metal fabrication and refining industry. The production of ethylene for industrial uses is one of the largest producers of anthropogenic $CO_2$ today. Greenhouse gas emissions from industrial processes generating ethylene surpasses that of the transportation industry by almost 50% [1]. Therefore, it is envisioned that large reductions in such anthropogenic carbon dioxide emissions from these industrial processes will be required to stabilize atmospheric concentration of greenhouse gasses [2]. Concordantly, substantial efforts have been made to find a suitable alternative method of production for ethylene. Ethylene is conventionally produced by steam cracking or heating natural gas containing ethane and propane to 800 - 900 Celsius which yields a mixture of gasses from which ethylene is separated.

Significant attention has been paid to carbon capturing techniques, such as oxy-fuel combustion systems, used to control the $CO_2$ emitted during power generation, commercial and residential heating, and in manufacturing. Chemical-looping-based oxidative dehydrogenation (CL-ODH) is a process that can be used to produce ethylene from ethane vastly more efficiently and safely than the traditional steam cracking processes [3]. Following the CL-ODH process, the resulting ethylene can be readily converted into liquid fuels via an oligomerization step. This novel gas to liquids process has several gaseous by-products; one of which is a mixture of gasses comprising different species including carbon dioxide, ethane, methane, carbon monoxide, water, ethylene, etc. [4]. As a result of these mixtures containing hydrocarbons, these by-product gasses have a considerable amount of energy that can be extracted and utilized to improve the overall efficiency of the CL-ODH process by converting the chemical energy in the fuel to electrical energy to power the plant and conversion process. Even though the CL-ODH process is a modern approach to clean production of ethylene that boasts thermal efficiencies of up to 96%, there is room for improvement so far as incorporating techniques to utilize the byproduct gasses [5]. The byproduct gas of concern has a concentration of 41% $CO_2$, 40% ethane, and 5% methane by weight with other minor compounds, which is represented in this work as a simulated (SIM) gas.

One of the easiest methods to efficiently utilize the SIM gas would be to combust the gases in an internal-combustion-engine based stationary generator due to the presence of hydrocarbons and the fuel pre-existing in a gaseous state. Since this fuel contains methane, a major species in natural gas fuel, performance and viability is expected to be similar to natural gas. In recent decades, natural gas combustion has been used as an alternative fuel in internal combustion engines to reduce the carbon footprint in the transportation, power generation, and other related industries [6]. Methane as a fuel has a high research octane of around 120 and a wide flammability range thus allowing operation in engines having compression rations greater than 12:1. Further, lean mixtures, such as those promulgated by methane provide enhanced knock resistance [7]. Therefore, in many ways using this fuel in an internal combustion engine can provide measurable advantages so far as thermal efficiency resulting from increased specific heat ratio, lower temperature of combustion, higher compression ratio, and decreased throttling losses. Spark ignition engines in use throughout the world, when operated on such natural gas fuels, often emit up to 50% fewer unburnt hydrocarbon emissions at WOT [8]. The biggest problem in using the fuel of concern in this work would be the presence of up to 45% $CO_2$ by weight in the gas byproduct. High concentrations of non-combustible $CO_2$ in the fuel mixture leads to a delay in the ignition and heat release, which is attributed to the increased heat capacity of $CO_2$ [9, 10]. In other words, the high concentration of carbon dioxide acts as a diluent of the fuel species which removes energy from the combustion event. In many ways this fuel is likened to a fuel charge subjected to high exhaust gas recirculation or EGR. Conventional EGR comprises a system to reintroduce inert products of combustion at a concentration of about 10% - 20% back into the intake to manipulate combustion and alter the products of combustion [11, 12].

Some of the issues of having a high concentration of $CO_2$ can be overcome by the mixture having high concentrations of ethane. Studies show that with increasing concentration of ethane in fuel mixture there can be a reduction in the ignition delay of the mixture [13]. The reduction in ignition delay is also dependent on the equivalence ratio of the fuel mixture [14-16]. The gas mixture also has a major portion of methane, which will also help in energy production. With a complex gas mixture as this there are much more complex mechanisms involved in the combustion process [15, 16]. Molecular ethane species in the mixture are very reactive and readily degrade into a more complex species in the chamber reducing the concentration of the primary fuel element. This degradation also affects the ability of methane to combust even more and thus increasing complexity in ignition [17, 18]. Previous studies have been performed on the same fuel mixture in a constant volume combustion chamber environment and the results concluded that while the mixture is harder to ignite, the performance of the fuel in an engine combustion scenario is viable with relative performance [19]. To better understand the effects of the fuel composition on the effectiveness of the fuel the emissions of the engine were recorded. In general, addition of natural gas or methane to the fuel mixture shows a reduction in the overall concentrations of carbon monoxide and nitrous oxides [20, 21]. The addition of $CO_2$ while simulating EGR, also reduces the flame temperature inside the combustion chamber helping with the control of emissions by the engine [22 - 24].

This study explores the efficacy of utilizing the byproduct gas resulting from the CL-ODH process in an internal combustion engine for stationary power generation. Further, the emissions characteristics of the fuel are also studied and compared against conventional fuels such as gasoline to identify the effectiveness of this fuel as a replacement or supplement to gasoline for power generation in internal combustion engines. Finally, the ability to modify and adapt existing internal combustion engines to use this fuel.

## 2. MATERIALS AND METHODS

A commercially available gasoline powered generator was instrumented and modified to conduct the experiments. Such a generator was chosen for these experiments primarily in order to simulate real world conditions more closely, as these fuels are being investigated for use in power generation in similar conventions. The engine used is an air cooled, single cylinder, four stroke spark-ignition engine with a displacement of 420 cc. It has a compression ratio of 8.3:1 and a bore and stroke of 90 mm x 66 mm. The engine has a push rod style single overhead cam valve arrangement and is fed via a single fuel circuit carburetor. When run on 87 octane or higher gasoline, the engine is capable of producing 10 kW and 25 N-m of torque at 3600 rpm. These engines are common in the art and are utilized in a variety of applications. Table 1 lists the specifications of the engine.

| Specification | Value |
|---|---|
| Engine displacement | 420 CC |
| Compression ratio | 8.3:1 |
| Bore x Stroke | 90 mm x 66 mm |
| Rated RPM | 3600 |
| Cooling type | Forced Air Cooling |
| Rated RPM | 3600 |
| Rated Power | 10 kW |

**TABLE 1:** SPECIFICATIONS OF ENGINE GENERATOR TEST STAND

A generator head comprising a series of heating elements, whose current and voltage could be measured, was adapted to provide constant load to the engine. To simulate this operational load, these electric heating elements were connected to the generator whereupon large iron castings were placed on the heaters to absorb the heat produced to ensure they could continuously provide load to the engine.

Several modifications were made to the engine intake to enhance its ability to operate with the gas supply. The most significant of these included a custom intake runner that was optimized for 3600 rpm operation, and 3D printed to adapt the gas mixing chamber to the carburetor. Constraints on this intake runner included retaining variability between mixed gas induction and regular air induction to the carburetor for conventional gas operation. A PVC accumulation chamber was installed above the engine and connected to the intake runner via a hose and a small port in the side of the chamber to properly mix the fuels. This chamber was used to create a homogeneous and thorough mixture of methane, ethane, and $CO_2$ prior to induction into the engine. The gases were fed into the accumulation chamber at 70 kPa gauge pressure. For the experiments with mixed gas, the carburetor was decommissioned, and the fuel lines were bypassed by the intake manifold so that no gasoline was introduced into the engine. Gasoline supplies were restricted as well to prevent interference from the fuel tank. Most generators are equipped with governor systems to ensure the engine operates as close to 3600 rpm as possible to provide constant 60 Hz. The governor works by limiting the ignition if the engine RPM varies too much. The governor was deactivated when testing the gas mixtures so the engine speed could be manually controlled by controlling the mass flow of mixed gasses.

The generator system was instrumented to record the parameters of the engine during operation. K-Type thermocouples were installed in a plurality of locations on the engine, including the cylinder head, exhaust, cylinder, crankcase, ambient, intake charge (premixed), and oil reservoir. A Bosch mass airflow (MAF) sensor was used to measure the quantity of air induced into the engine continuously. The 3D printed intake runner was modified to adapt the MAP sensor to monitor intake manifold pressure. A Kistler model 6052A piezoelectric pressure transducer was installed into the cylinder head to measure in-cylinder pressure as shown in Figure 1. To measure the exhaust emissions, an Infrared Industries FGA 4000XDS exhaust gas analyzer was used in the exhaust stream. The exhaust analyzer used NDIR (non-dispersive infrared) to measure UHC, CO, and $CO_2$ species. The analyzer also used an electrochemical cell to measure the $NO_x$ emissions within a 1% full-scale accuracy. On the end of the engine, a gearbox assembly was mounted to the crankshaft which contained a Hengstler 0521097 shaft encoder that was used in combination with a MP1007 Hall effect sensor to accurately determine crank angle position, top dead center, and RPM of the engine. Finally, a Bosch intake manifold pressure sensor was installed to the intake track to monitor the pressure drop of the fuel charge as it entered the engine. Data from each sensor was collected with a bespoke LabVIEW program; the program was used to record the data and synchronize the signals. Further, the LabVIEW program was also used to control the flow of the gasses. From there, the data was analyzed with MATLAB. The systems deliver reliable measurement results with an accuracy of 5% based on the least accurate instrument. To supply the fuel, bottles of each gas were connected to the accumulator and controlled with Brookfield electronic mass flow controllers. Once the gas was mixed via the accumulator, it was throttled into the intake via the carburetor. On this engine, the throttling was accomplished automatically via the centrifugal governor on the engine connected to the carburetor. During gasoline operation, the carburetor assumed standard function. For mixed gas operation, gasoline flow was blocked off and residual gasoline was drained. Further, the orifices were blocked such that the carburetor only functioned as a throttling apparatus. Apart from these modifications, all other engine parameters such as timing, A/F ratio, etc. were held constant. An A/F ratio of 19.2, 19.6, and 19.8 was used for the gas mixtures 1, 2, and 3 respectively and an A/F ratio of 13.2 was used with gasoline. Corresponding equivalent ratios were .97 for Mix-1 and .96 for Mix-2 and Mix-2. As a result of utilizing the carburetor, gasoline operation was fuel rich having an equivalence ratio of 1.11

Several modifications were necessary to measure the amount of fuel used for each of the fuel types. For gasoline, the gas tank was bypassed with a fuel inlet line to the carburetor fed by a graduated container. The engine was first run with no gasoline in the container to dry out the carburetor bowl and make sure that there is no fuel in the lines. Once the engine stalled, the container is filled to a specific level and the flow valves are opened. Then the engine was started, and the test case was run while time is recorded to exhaust the supply of fuel. Because the gaseous fuel mixtures were controlled by calibrated mass flow controllers, the outputs of the controllers were taken as the fuel consumption over time.

For this study different load conditions were tested to understand the performance of the fuels.. For full load, a series of electrical heaters with 5.2 kW of power output were used to electrically load the generator to its rated continuous power output. Part load was tested with fewer electrical heaters which provided 3.2 kW of power output. No load was tested without any external electrical load attached to the generator and only energizing the coils of the generator and the internal control circuitry. Due to uncertainties in the performance of the connected generator, the indicated power was calculated from the calculated indicated mean effective pressure (IMEP). Prior to testing the gas mixtures, a series of experiments were conducted with gasoline to establish a baseline with which to compare the gas mixture performance. The gasoline was obtained from a local gas station and was 90-octane non-ethanol. The efficiency and emissions of the pure gasoline case were measured and tabulated to establish baseline results. The tests performed were repeated 15 times with the same setup to test repeatability and eliminate errors, and the data was taken as an average of 10 continuous minutes of running at a fixed load and RPM for each test. The variation bars in the graphs show the standard deviation for the data presented. After the gasoline cases were conducted, varying mixtures of methane, ethane, and $CO_2$ were used as fuel based on the outputs of the CL-ODH process. The ratios of methane, ethane, and $CO_2$ tested are shown in Table 2. The mixtures shown in Table 2 were chosen based on their resemblance to the original byproduct gas from the CL-ODH process as they closely resemble the variety of the byproduct mixture.

Due to the complex nature of the original byproduct gas, a simulation gas with the major components was employed based on the study in a constant volume combustion chamber to identify the mixtures with the highest likelihood of being viable for use in an engine application [19]. This simulation was set up in Converge-CFD™ and included modified solvers with detailed chemistry to model the combustion of the byproduct gasses. The initial cases were used to simplify the fuel mixture to reduce the complexity of the SIM gasses prior to testing. A series of simplified gases were compared against the original gas to ensure that the SIM gas was authentic. It is important to consider carbon dioxide does not contribute to the lower heating value calculation because carbon dioxide does not contribute any energy. Based on the simulation, ethane, and methane were identified to have the largest influence in the heat release of the fuel. As a result of the experiments, it was possible to eliminate the minor species and develop simulated gas mixtures consisting essentially of methane, ethane, and $CO_2$. By eliminating the minor species, it is possible to dramatically increase the ease of experimentation while maintaining a good match to the actual fuel. Table 3 shows the lower heating value of the fuels used for each of the loading conditions tested.

| Mix | Wt. % Ethane | Wt. % Methane | Wt. % $CO_2$ |
|---|---|---|---|
| Mix-1 | 46 | 12 | 42 |
| Mix-2 | 46 | 10 | 44 |
| Mix-3 | 47 | 7 | 46 |

**Table 2:** FUEL MIXTURE RATIOS USED IN THE EXPERIMENTS IN WEIGHT %

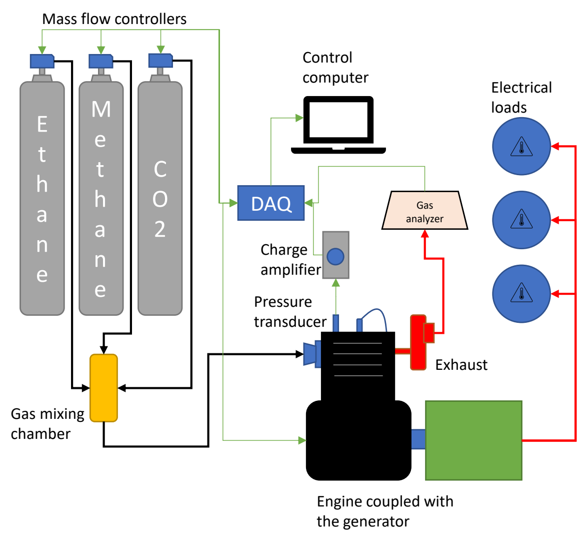


**FIGURE 1:** SCHEMATIC OF THE EXPERIMENTAL SETUP SHOWING THE GAS INDUCTION SYSTEM

## 3. RESULTS AND DISCUSSION

### 3.1 In-cylinder combustion comparison

The pressure transducer installed on the cylinder head provided the transient combustion pressure inside the combustion chamber. The data collection was synced to the rotation of the engine to obtain the pressure data as a function of crank angle. This pressure data was then used to calculate the indicated mean effective pressure (IMEP). Indicated mean effective pressure is a quantity which relates the internal combustion engine to its capacity to do work. Significantly, this measurement quantifies engine performance independent of engine displacement.

Figure 2 shows a plot containing the in-cylinder combustion pressure vs. crank angle degree at varying loads. From Figure 2, it is observed that the peak pressure for Mix-2 and gasoline are very close and almost overlap. It was also shown that the Mix-1 shows a higher peak, because of the highest concentration of fuel components and lowest concentration of diluent $CO_2$. Under full load, the fuels effects on combustion pressure are considered significant with more than 10% difference. The increased ratio of methane in the fuel mixture coupled with the lowest ratio of $CO_2$ is responsible for this high peak pressure resulting from gaseous fuels having a higher heating value. Lower concentrations of $CO_2$ also reduce the energy absorbed by the diluent species. Conversely, with Mix-3 having the most $CO_2$ in the fuel, the mixture shows the lowest peak pressure. Similar trends are seen with all the loads tested with the fuels.

| Fuel | LHV (MJ/kg) excluding $CO_2$ | LHV (MJ/kg) |
|---|---|---|
| **Mix-1** | 47.6 | 27.7 |
| **Mix-2** | 47.5 | 26.7 |
| **Mix-3** | 47.4 | 25.7 |
| **Gasoline** | - | 43.4 |

**Table 3:** LOWER HEATING VALUES OF THE FUEL MIXTURES TESTED

When comparing part load to full load, it is observed that the differences between each of the fuels is much less significant. It is important to note that the peaks' location relative to diluent content is consistent throughout loading conditions; increasing amounts of diluent leads to a lower in-cylinder pressure. Mix-1, having the greatest energy content, continues to demonstrate the highest peak pressure and Mix-3, having the lowest energy content, shows the lowest peak pressure. Mix-1 shows the greatest decrease in in cylinder pressure when engine operation is reduced to part load. Continuing to comport with the trends from full to part load, the discriminable differences between each fuel diminishes further when considering no load, and the relationship between diluent and in-cylinder pressure continues to be maintained. It is important to consider that each of the fuels exhibit similar performance to gasoline at no load situations, which is most likely due to heavy throttling at no load.

Using the IMEP results, the indicated power produced by the engine at the various loading conditions can be calculated using the following equation [25]:

$$P_i\ (kW) = \frac{IMEP * Vd * N}{2 * 10^3} \tag{1}$$

where $P_i$ is the indicated power, $V_d$ is the displaced volume, and $N$ is the rotational speed of the engine in revolutions per second. Table 4 shows the calculated indicated power for different load conditions. Note that the achieved max loading on the engine is lower than the rated power of the engine. While the engine is rated for 10 kW, the generator is only able to supply 75% of the rated load during continuous load operation, reserving full power for surge operation. This safety feature is incorporated to prevent overloading of the generator.

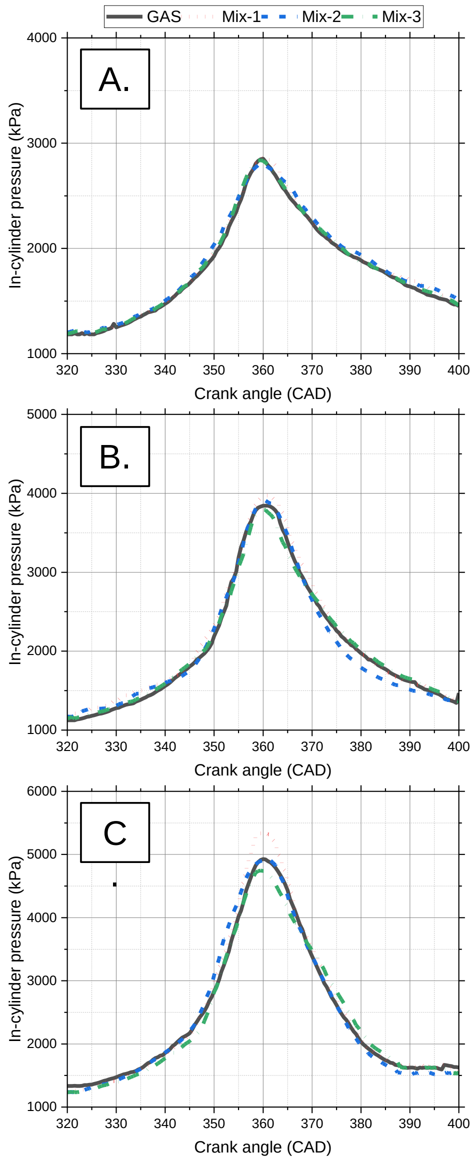


**FIGURE 2:** IN-CYLINDER PRESSURE COMPARISON A. NO LOAD, B. PART LOAD, C. FULL LOAD

Using the in-cylinder pressure data, the heat release rate (HRR) of the combustion cycles was also calculated and analyzed. The heat release rate is critical in understanding the combustion characteristics of the fuel because it can describe fuel burning rate. The heat release rate was calculated using the first law heat release model as shown in Equation 2, with $\gamma$ (a value of 1.325 is used) being the specific heat ratio [25].

$$\frac{dQ}{d\theta} = \frac{\gamma}{\gamma-1} P \frac{dV}{d\theta} + \frac{1}{\gamma-1} V \frac{dP}{d\theta} \tag{2}$$

| Indicated power kW | Gasoline | Mix-1 | Mix-2 | Mix-3 |
|---|---|---|---|---|
| No-load | 1.07 | 1.16 | 1.12 | 1.08 |
| Part-load | 5.70 | 6.01 | 5.83 | 4.95 |
| Full-load | 7.98 | 8.81 | 7.99 | 7.22 |

**Table 4:** CALCULATED INDICATED POWER GENERATED BY THE ENGINE WITH DIFFERENT FUELS AND LOADS

In a similar way to in cylinder pressure, the heat release rate between the fuels was compared. Comparing the heat release rate to the crank angle further develops an understanding of fuel burning behavior and fuel viability as a replacement for gasoline. Figure 3 shows the comparison between heat release rate at varying load conditions.

When comparing heat release rates, slightly different trends are observed between loading conditions. As load increases, the differences between the mixtures increases. Conversely to in cylinder pressure trends, however, it was observed that Mix-1, whose energy content is the greatest among the three mixtures, shows the lowest heat release at low loads. As loading increases, the heat release rate increases more rapidly than any other mixture. At high load operation, Mix-1 demonstrates a heat release rate that is higher than any mixture.

Mix-2 demonstrates a heat release rate closest to that of gasoline in terms of peak heat release rate under all loading conditions, further suggesting that it may operate as a viable replacement for gasoline. Despite this close match in absolute heat release, the heat release event extends over a slightly longer duration. Mix-3 exhibits the lowest heat release rate. This low heat release rate, as is the case with low in cylinder pressure, is a result of containing the greatest concentration of $CO_2$ diluents which absorb heat from combustion. The heat release rate of Mix-3 continues to diminish relatively lower when compared to other mixes and gasoline as load increases. Another discrepancy between the fuels that should be noted is peak of the heat release rate curve compared between the mixes. When compared to Gasoline, Mix-1 is most closely aligned, indicating that peak heat release occurs at similar CAD. Mix-2 has the broadest curve indicating that the heat release rate is sustained over a greater duration.

Figure 4 shows the peak heat release rate results for different engine loads and fuel mixtures. From Figure 4, the gas mixtures show a difference based on the mixture condition being tested. At the no load condition all the fuels tested show similar peak HRR. But Mix-1 shows a marginally higher heat release rate compared to others. A similar trend is observed with the other loading cases as well, where the Mix-1 has the highest HRR. As the load increased to full load, it was noticed that the difference increased between each fuel mixture tested. Mix-2 is quite close to the performance of gasoline. Mix-3 proves to be the slowest burning among all the fuels due to its highest $CO_2$ concentration. The heat release from the gas mixtures is a consistent match to gasoline. Even in light of the varying heat release rates demonstrated by these fuels, it can be argued that the heat release rate of the fuels is sufficient for the fuel to be utilized in an internal combustion engine. Table 5 shows calculated combustion duration and combustion rate (*i.e.*, average heat release rate), which is based on the mass burning fraction (MBF) from 10% to 90% using the heat release data. From Table 5, it is shown that the combustion duration for the SIM fuels is similar to gasoline.

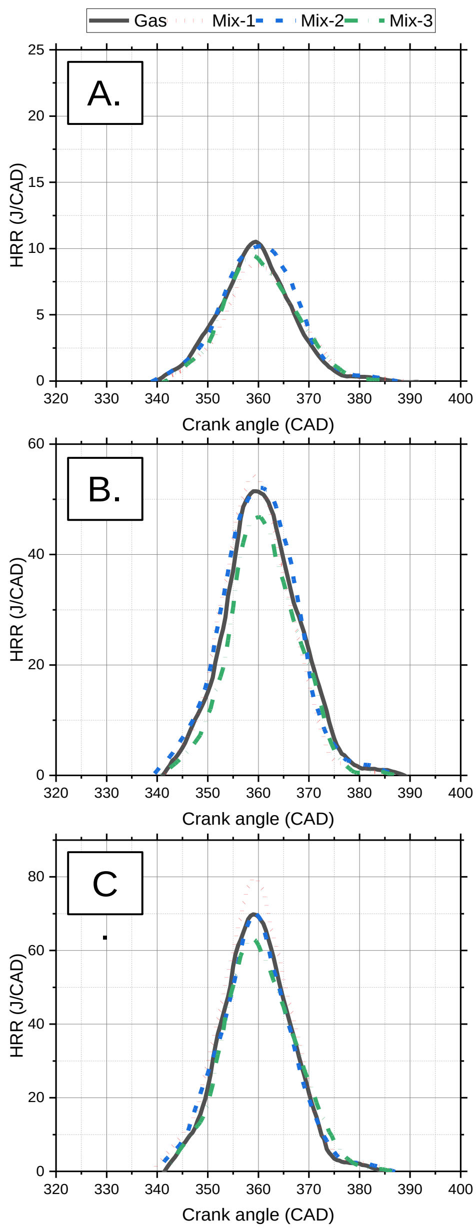


**FIGURE 3:** HEAT RELEASE RATE COMPARISON AT FULL LOAD BETWEEN FUELS A. NO LOAD, B. PART LOAD, C. FULL LOAD

| Combustion Duration (CAD) | Gasoline | Mix-1 | Mix-2 | Mix-3 |
|---|---|---|---|---|
| No-load | 17.98 | 18.12 | 18.61 | 18.61 |
| Part-load | 18.24 | 18.37 | 18.48 | 18.78 |
| Full-load | 18.54 | 18.68 | 18.81 | 18.95 |
| Combustion Rate (J/CAD | Gasoline | Mix-1 | Mix-2 | Mix-3 |
| No-load | 7.10 | 7.07 | 6.94 | 6.87 |
| Part-load | 41.37 | 41.91 | 41.31 | 37.04 |
| Full-load | 53.15 | 59.05 | 50.34 | 47.83 |

**TABLE 5:** CALCULATED COMBUSTION DURATION AND RATE

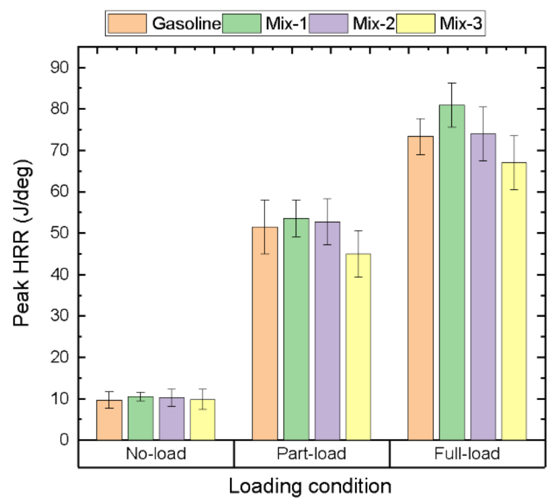


**FIGURE 4:** PEAK HEAT RELEASE RATE COMPARISON BETWEEN FUELS FOR ALL LOADING CONDITIONS

### 3.2 Fuel efficiency comparison

With the power measured, the indicated efficiency can be calculated. Indicated efficiency is defined as the ratio between indicated power and the chemical energy provided by the fuel, also known as indicated fuel conversion efficiency. The formula below was used to calculate fuel conversion efficiency [25].

$$\varepsilon = \frac{P_i}{Q_{hv} * \dot{m}_{fuel}} \tag{3}$$

where $Q_{hv}$ are the lower heating values of the fuel and $\dot{m}_{fuel}$ is the mass flow rate of the fuel. Figure 5(shows the energy equivalent mass of gasoline consumed per kilowatt hour generated for the various fuels mixtures and loads tested. The calculation and conversion of fuel consumption values shown in Figure 4 includes only the combustible gasses in the gas mixtures tested. The mass of $CO_2$ has not been accounted for here as it does not contribute to releasing any energy through combustion. The fuel consumption calculations are also based on the indicated power calculated from IMEP measurements. Figure 5, which demonstrates indicated fuel conversion efficiency, shows at lower loads gasoline fuel tests show reduced fuel consumption compared to gas mix cases even though the gasses have higher chemical energy in the fuel. Gas Mix-3 also shows the highest specific fuel consumption per cycle of all the gaseous mix fuels tested, which is expected as it contains the lowest number of hydrocarbons and greatest concentration of carbon dioxide. With an increase in loading, the fuel consumption for gaseous mixture fuels reduces and then increases slightly. Overall, Mix-1 with its increased methane concentration shows a good reduction in fuel consumption at mid to high loading conditions compared to all the gaseous fuels tested. Considering the uncertainty, the difference in fuel consumption is minor under part and full loads.

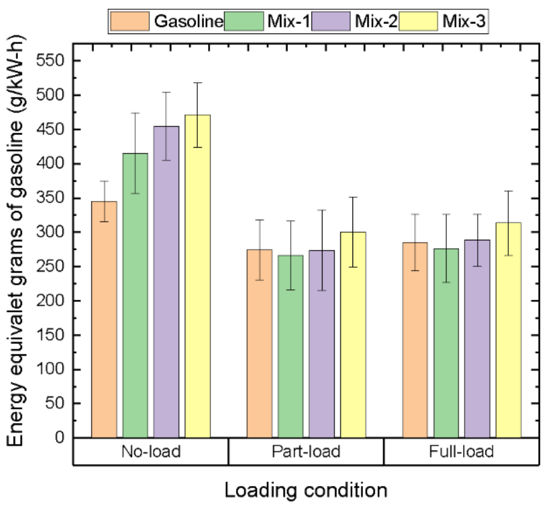


**FIGURE 5:** INDICATED FUEL CONSUMPTION COMPARISON FOR ALL THE FUELS AND LOADS TESTED. VALUES REPORTED ARE IN ENERGY EQUIVALENT MASS OF GASOLINE FOR ALL THE FUELS ($CO_2$ IS EXCLUDED FROM THE MASS OF FUEL FOR THIS CALCULATION)

Figure 6 illustrates the indicated fuel conversion efficiency for all the conditions. From Figure 6, it can be seen that the indicated efficiency of the engine follows different trend when compared to fuel consumption for all the loads. The no-load condition shows that the gasoline engine has a relatively higher indicated efficiency as compared to the gas mixtures. This effect can be attributed to the system used to induce the gas mixture into the engine. For gasoline, the carburetor was unmodified, and the throttle was adjusted and fixed to run the engine at 3600 rpm based on the load applied. But for the gas mixtures, the overall control of the fuel mass entering the chamber was accomplished by strictly controlling the flow rate of individual gasses being fed into the mixing chamber, which empties out into the intake of the engine. As a result of intake and induction inefficiencies and based on mass flow measurements , the engine required a considerable influx of gas to keep it running at idle or with no loads, most of which was ultimately lost to the atmosphere and never entered the engine. The overall trend of the reduction in efficiency with the changing mixture properties remains the same between the gas mixtures. It should be noted that improvements to the gas induction system and throttling mechanism would decrease the fuel consumption of the mixed gasses.

The data suggests the highest indicated efficiency is from using gasoline rather than from using the mixed gasses. Although EGR systems and fuels of the like are appealing for their ability to reduce emissions, they have detrimental effects on fuel efficiency [12]. These facts are evident in light of comparing gasoline to the SIM fuels which mimic EGR behavior.

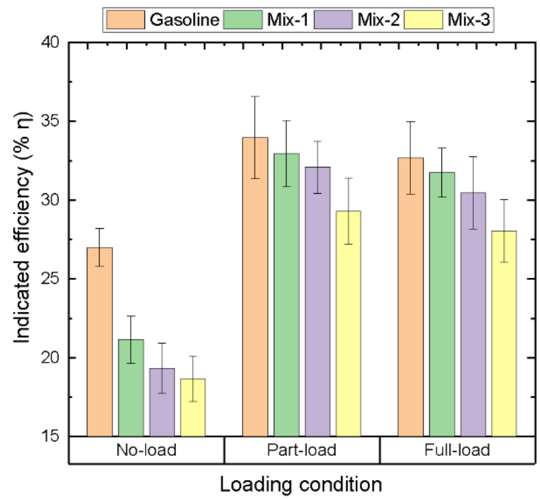


**FIGURE 6:** EFFICIENCY COMPARISON FOR THE FUEL MIXTURES UNDER VARYING LOADS

Mix-1 shows a better indicated efficiency compared to the mixed gasses across the board as it has the least amount of $CO_2$ dilution compared to the three mixtures. Similarly, Mix-3 suffers from the lowest indicated efficiency of all as it has a higher $CO_2$ dilution. As the $CO_2$ dilution increases, the indicated efficiency decreases. This is a result of the $CO_2$ absorbing energy from the combustion process. More fuel is then required to replace the lost heat. Further, the reduction in indicated fuel conversion efficiency for the gas mixtures is also because of increased $CO_2$ concentration leading to slower combustion and lower combustion temperature. At part load there is only a 3% difference between gasoline and the Mix-1 gas, 6% between gasoline and Mix-2, and 14% between gasoline and Mix-3. The difference reduces further with increasing loads. Consider that as load increases, cylinder filling and volumetric efficiency often increases. [25]. Thus, it is likely this difference decreases as load increases because of the increased turbulence and decreased throttling losses experienced during lower load operation. The efficiency of the gas fed systems can possibly be further improved by the modification of the fuel induction system and improving the mixture homogeneity of the gasses being fed into the engine.

### 3.3 Exhaust gas analysis

In this study the exhaust temperature and gasses from the engine were sampled and tested to analyze the emissions and understand combustion characteristics for each of the SIM gasses using a calibrated exhaust analyzer. First, the exhaust gas temperature was sampled. Next, the exhaust was sampled to measure quantities of unburnt hydrocarbons (HC), carbon monoxide (CO), carbon dioxide ($CO_2$), and oxides of nitrogen ($NO_x$). All the emissions data shown are in units of grams per indicated kilowatt hour (g/kW-h) for accurate comparison.

### 3.3.1 Exhaust temperature

Exhaust gas temperature (EGT) is critical in understanding the combustion event; in many cases EGT can indicate a rich or lean condition [25]. Further, monitoring EGT is important to ensure that the mixed gasses are not exceeding the safe limits of engine design. Catastrophic engine failure often results from exhaust gas temperatures exceeding these designed limits. Thus, it is critical to understand exhaust gas temperature when evaluating the compatibility of this fuel in an engine.

Although EGT can be influenced by a variety of engine parameters such as ignition timing and engine tuning, these are neglected for this study because they are all held constant; consider that exhaust gas temperature is primarily influenced by the combustion behavior and stoichiometry of the fuel charge [14]. Figure 7 shows the variation in exhaust gas temperature for the different fuels tested under different loads. It can be seen that the exhaust temperature for the fuel Mix-3 is the lowest. Lower EGTs can be the result of variation of the A/F ratio and by less energetic combustion [25]. In this case, it could be caused by the increased $CO_2$ absorbing more heat inside the chamber and in the exhaust of the engine. Mixtures with lower exhaust gas temperatures indicate the combustion event corresponds to fuel that has a lower adiabatic flame temperature. As load increases, the exhaust gas temperature increases as a result of more fuel being consumed and higher cylinder combustion temperature.

### 3.3.2 Unburnt hydrocarbon (UHC) emissions

Figure 8 shows the UHC emissions for different fuel mixtures and loads tested. Results show that the UHC emissions for gasoline is considerably lower than that of any gas mixtures tested. This could be due to the relatively slower combustion of the gas mixtures as identified in tests of said mixtures in a constant volume combustion chamber [19]. This slower combustion can cause some of the induced gasses to not completely combust and exit out through the exhaust causing an increase in the overall UHC levels. Another reason could be that there is a possibility of the induced gas mix being locally richer inside the combustion chamber causing some unburnt gasses to be exhausted out and increase the overall UHC levels. A better control of the induced gas mixture may help reduce the overall UHC emissions when using the gas mixtures as fuel.

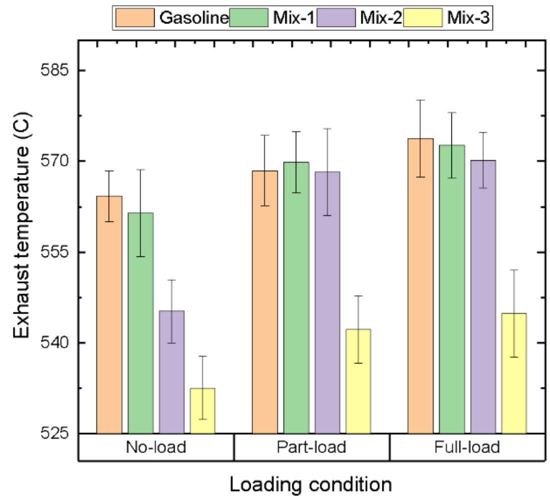


**FIGURE 7:** EXHAUST TEMPERATURE VARIATION WITH DIFFERENT FUELS AND LOADS

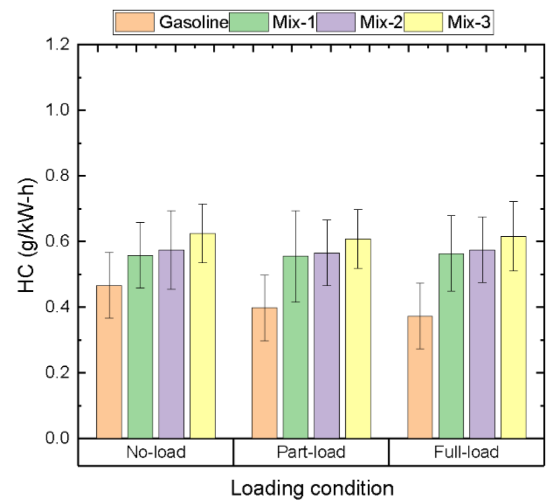


**FIGURE 8:** HC EMISSION COMPARISON FOR ALL THE FUELS AND LOADS SHOWN IN GRAMS PER INDICATED KILOWATT HOUR

### 3.3.3 Carbon Monoxide (CO)

Figure 9 shows the CO emissions for different fuels and loads. For CO emissions, a trend that is essentially opposite to the HC emissions can be observed, where the gasoline system emits approximately twice the amount of CO at higher loads compared to the gas mixtures. This is likely the result of the fuel/air mixture becoming richer as load increases. The relatively high flame temperature of the induced gas mixtures could also help in burning the CO species, leading to a reduction in the overall CO levels.

### 3.3.4 Carbon Dioxide ($CO_2$)

Figure 10 shows the relative amount of $CO_2$ emissions produced by each fuel. $CO_2$ production for all the fuels remains close to each other; there is an increase of $CO_2$ emissions with increasing loads for all the fuels. But at all loads the gas mixture fuels exhaust more $CO_2$ compared to gasoline. Mix-3 consistently has the highest $CO_2$ as it has the highest $CO_2$ in the mixture. The $CO_2$ emissions produced by the fuels are directly proportional to the amount of $CO_2$ in the fuel. When compared to gasoline, the SIM fuels have substantially more carbon dioxide. This increase in $CO_2$ is a result from the introduced carbon dioxide as part of the fuel that ends up as emissions from the engine, which increases the overall $CO_2$ levels in the exhaust. An argument could be made that the $CO_2$ emitted is a combination of products of combustion and fuel constituents, where the $CO_2$ introduced as fuel should be represented with different weight than that of a product of combustion. It is likely that the $CO_2$ emissions that are products of combustion from the SIM gas are of substantially less quantity than that produced from gasoline. Because the SIM gas contains $CO_2$, there will be higher than atmospheric concentrations of $CO_2$, which is typically .041%. Further, there will be an increased concentration from the same. Table 6 gives the measured $CO_2$ concentration of the intake and exhaust. It should be noted that the exhaust $CO_2$ concentration is dry based.

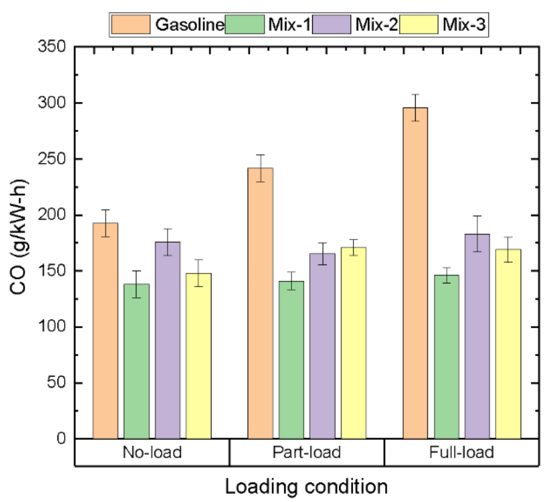


**FIGURE 9:** CO EMISSION COMPARISON FOR ALL FUELS AND LOADS SHOWN IN GRAMS PER INDICATED KILOWATT HOUR

| **%(pre/post) $CO_2$,** | No Load | Part Load | Full Load |
|---|---|---|---|
| Mix-1 | 5.31 / 19.5 | 5.33 / 23.5 | 5.30 / 24.3 |
| Mix-2 | 5.41 / 20.5 | 5.43 / 25.2 | 5.44 / 25.4 |
| Mix-3 | 5.56 / 21.3 | 5.55 / 26.1 | 5.54 / 27.0 |

**Table 6:** $CO_2$ CONCENTRATIONS FROM INTAKE AND EXHAUST

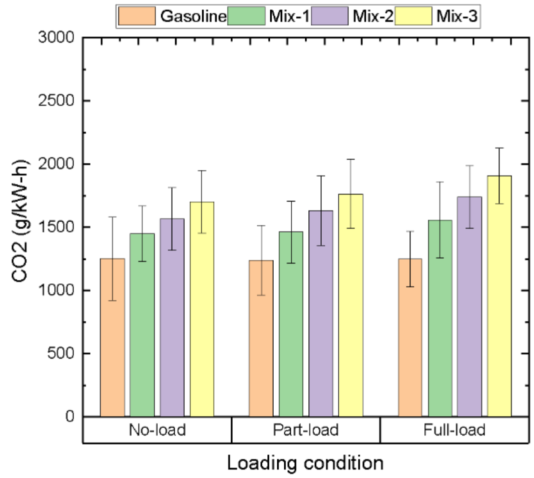


**FIGURE 10:** $CO_2$ EMISSION COMPARISON FOR ALL FUELS AND LOADS SHOWN IN GRAMS PER INDICATED KILOWATT HOUR

### 3.3.5 Oxides of Nitrogen (NOx)

NOx emissions in IC engines are mainly influenced by the temperature of combustion inside the chamber. On its face, it is expected that these gas mixtures would emit lower $NO_x$ emissions resulting from the lower temperatures within the cylinder from the heat removed by the $CO_2$. These presumptions are somewhat consistent with the measurements taken, but more analysis is required. Figure 11 shows the $NO_x$ levels for different fuels and the loading conditions tested. From Figure 11, it can be seen that the $NO_x$ emissions for the gasoline cases generally increase with the increase in the load applied to the engine. This is due to the increase in the combustion temperature under higher loads coupled with a warmer engine. The increasing temperature of combustion also indirectly heats the engine to a higher temperature at higher loads causing the inlet charge to be hotter. This phenomenon can also increase the overall $NO_x$ production in the exhaust. But with the gas mixtures the $NO_x$ initially increases and then almost stagnates. Since the gasses that are used are in a mixing chamber and forced into the inlet of the engine, the mixture stays relatively cooler. This reduces the amount of $NO_x$ produced. Reiterating, the increased $CO_2$ in the fuel mixture helps in absorbing some of the energy that leads to a lower flame temperature with less thermal $NO_x$ formation.

### 3.4 Engine mechanical health analysis

It is common when investigating alternative fuels to consider the effects these unconventional fuel extract on an engine. Several parameters, such as corrosivity and heat quenching should be considered when evaluating whether an alternative fuel is suitable for use in an engine designed for conventional gasoline or diesel operation as such characteristics influence the reliability of an engine. For this study the mechanical health of the engine was evaluated prior to and post operation of the gas mixtures.

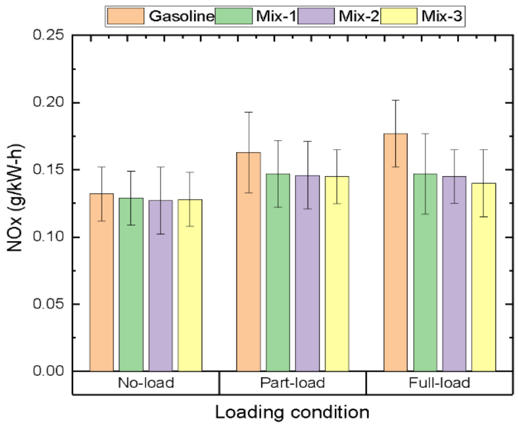


**FIGURE 11:** NOx EMISSION COMPARISON FOR ALL FUELS AND LOADS SHOWN IN GRAMS PER INDICATED KILOWATT HOUR

A compression test is normally performed to quantify the mechanical integrity of a cylinder and combustion chamber on an internal combustion engine whereby it measures the static pressure developed during compression. Low compression is indicative of poor mechanical health resulting from wear. A compression test was performed on the engine when it was new and after extensive operation on the fuels and on gasoline. The initial compression test indicated 118 psi, and the subsequent test indicated 116 psi. This loss of 2 psi is negligible and can be attributed to normal "break in" or wear from extended operation. In other words, there was no accelerated decline in compression experienced by the engine resulting from SIM gas operation. If there were a negative phenomenon, such as auto ignition, detonation, flame quenching, overheating, etc. it would have damaged the cylinder, head, and valvetrain and cause a detectable loss of compression.

A series of qualitative engine assessments were performed to further strengthen the assessment of minimal impact from these fuels. Melting may also occur by combustion events that are relatively slow which increase the resonance time of the flame. Figure 12 shows an image of the cylinder head after experimentation.

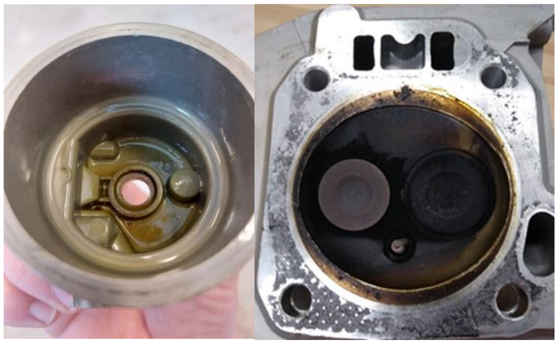

**FIGURE 12:** IMAGE OF CYLINDER HEAD AND CARUBUERATOR AFTER EXPERIMENTATION

From the image in Figure 12, it can be assumed that no such damage occurred from inconsistent or unfavorable combustion. It is also common with the introduction of certain unconventional fuels for chemical reactions to occur resulting in the corrosion of internal parts. Exemplary interactions include ammonia-brass reactions when ammonia is used as a fuel, and it reacts with the brass items in the fuel intake. The carburetor was disassembled and inspected for such interactions. Figure 12 contains an image of the carburetor after the experiments were performed. From the image in Figure 12, it is evident that no such corrosion exists from adverse reactions from the fuels or any of their products. Further testing is required to understand the complete effects of these fuel on existing internal combustion engines.

Overall, the experiments and results in this work suggest the gas mixtures show improvement in CO and NOx emissions when compared to gasoline. It was also shown that the fuel can be operated in existing spark ignition internal combustion engines without substantial internal modifications. Consider that an intake system similar to the one used in this work could be improved upon to provide finer control over the mixtures to reduce slight variations and be commercialized and mass produced. Further, after mixed gas operation, it was concluded that there were no adverse effects on engine health because of operating on mixed gas. It should be noted, however, that long term studies on engine health should be conducted.

## 4. CONCLUSION

Simulated gas mixtures, which modeled the byproducts of the CL-ODH processes, were tested in a spark ignition engine to evaluate the combustion, performance, and emissions, and to understand its compatibility in existing internal combustion engine-based power generation units with little modifications. It was concluded that the gas mixture can be used in spark-ignition engines with slight modifications to the intake system and produce little to no side effects. Further, the engine can be cycled between mixed gas mode and conventional gasoline operation with no adverse effects. It was found that at higher loads, the simulated gas mixture shows between 6% to 16% lower thermal efficiency than gasoline. It is likely that this is the result of higher concentration of diluents in the fuel. When compared to gasoline, the byproduct gas mixtures yield lower CO and NOx emissions; at higher loads, the byproduct gas mixtures demonstrated up to 41% reduction in CO and up to 21% reduction in NOx. This substantial improvement in harmful emissions increases the attractiveness of the use of the fuel in stationary power generation settings. For steady load applications, it is seen that the byproduct gas mixtures can be successfully used in an engine with similar performance. Further improvements of the overall performance may be done with modifications and optimization to the intake system to decrease the amount of fuel lost and the consistency of fuel delivery.

**ACKNOWLEDGEMENTS**

This work was supported in part by the US Department of Energy (RAPID Sub-award DE-EE0007888-05-6). Any opinions, findings, and conclusions or recommendations expressed in this material are those of the author(s) and do not necessarily reflect the views of the funding agencies.

**REFERENCES**

[1] Environmental Protection Agency. (n.d.). Global Greenhouse Gas Emissions Data. EPA. Retrieved March 17, 2022.

[2] de Persis, S., Foucher, F., Pillier, L., Osorio, V., and Gökalp, I. (2013). Effects of O2 enrichment and CO2 dilution on laminar methane flames. Energy, 55, 1055-1066.

[3] Neal, L.M., Yusuf, S., Sofranko, J.A., Li, F., Oxidative dehydrogenation of ethane: a chemical looping approach. Energy Technology. 2016 Oct; 4(10):1200-8.

[4] Neal, L.M., Haribal, V.P., Li, F., Intensified Ethylene Production via Chemical Looping through an Exergetically Efficient Redox Scheme. iScience. 2019 Sep 27; 19:894-904.

[5] Brody, L., Neal, L., Haribal, V., and Li, F. (2021). Ethane to liquids via a chemical looping approach–Redox catalyst demonstration and process analysis. Chemical Engineering Journal, 417, 128886.

[6] Baratta, M., Chiriches, S., Goel, P., and Misul, D. (2020). CFD modelling of natural gas combustion in IC engines under different EGR dilution and H2-doping conditions. Transportation Engineering, 2, 100018..

[7] Nitta, Y., Yoo, D. H., Nishio, S., Ichikawa, Y., Hirata, K., and Yamasaki, Y. (2016, October). Evaluation of emissions characteristics by charging exhaust gas from lean burn gas engine into marine diesel engine. In Internal Combustion Engine Division Fall Technical Conference (Vol. 50503, p. V001T04A002). American Society of Mechanical Engineers.

[8] Cho, H. M., and He, B. Q. (2009). Combustion and emission characteristics of a natural gas engine under different operating conditions. Environmental Engineering Research, 14(2), 95-101.

[9] Shudo, T., Kitahara, S., and Ogawa, H. (2006). Influence of carbon dioxide on combustion in an HCCI engine with the ignition-control by hydrogen (No. 2006-01-3248). SAE Technical Paper.

[10] Karim, G. A., and Wierzba, I. (1992). Methane-carbon dioxide mixtures as a fuel (No. 921557). SAE Technical Paper.

[11] Rao, A., Wu, Z., Mehra, R. K., Duan, H., and Ma, F. (2021). Effect of hydrogen addition on combustion, performance and emission of stoichiometric compressed natural gas fueled internal combustion engine along with exhaust gas recirculation at low, half and high load conditions. Fuel, 304, 121358.

[12] Mohr, J., Zdanowicz, A., Tryner, J., Gustafson, K., Venegas, J., Windom, B., ... and Marchese, A. (2019). Ignition, Flame Propagation, and End-Gas Autoignition Studies of Natural Gas/EGR Blends in a Rapid Compression Machine. (2019).

[13] Holton, M. M., Gokulakrishnan, P., Klassen, M. S., Roby, R. J., and Jackson, G. S. (2010). Autoignition delay time measurements of methane, ethane, and propane pure fuels and methane-based fuel blends. Journal of Engineering for Gas Turbines and Power, 132(9).

[14] Hashemi, H., Jacobsen, J.G., Rasmussen, C.T., Christensen, J.M., Glarborg, P., Gersen, S., van Essen, M., Levinsky, H.B., Klippenstein, S.J., High-pressure oxidation of ethane. Combustion and Flame, 182 (2017), pp. 150-166.

[15] Yossefi, D., Ashcroft, S.J., Hacohen, J., Belmont, M.R., Thorpe, I., Combustion of methane and ethane with CO2 replacing N2 as a diluent. Volume 74, Issue 7, 1995, Pages 1061-1071, ISSN 0016-2361,

[16] Liu, Y., Cheng, J., Zou, C., Lu, L., Jing, H., Ignition delay times of ethane under O2/CO2 atmosphere at different pressures by shock tube and simulation methods. Combustion and Flame. 2019 Jun 1; 204:380-90.

[17] Hu E., Chen Y., Zhang Z., Li X., Cheng Y., Huang Z., Experimental study on ethane ignition delay times and evaluation of chemical kinetic models. Energy Fuels, 29 (2015), pp. 4557-4566.

[18] Huang, J., Crookes, R.J., Assessment of simulated biogas as a fuel for the spark ignition engine, Fuel, Volume 77, Issue 15, 1998, Pages 1793-1801, ISSN 0016-2361,

[19] Vinod, K. N., Gore, M., Lee, A., Neal, L., Li, F., and Fang, T. Combustion and flame analysis of byproduct fuel mixture with high CO2 dilution from the Cl-ODH process of ethane to ethylene conversion. In 2020 Spring Technical Meeting of the Eastern States Section of the Combustion Institute, 2020.

[20] Malenshek, M., and Olsen, D. B. (2009). Methane number testing of alternative gaseous fuels. Fuel, 88(4), 650-656.

[21] Cho, H. M., and He, B. Q. (2009). Combustion and emission characteristics of a natural gas engine under different operating conditions. Environmental Engineering Research, 14(2), 95-101.

[22] Shi, Y., Jia, Y., Pan, W., Huang, L., Yan, J., and Zheng, R. (2017). Potential evaluation on CO2-EGR in tight and low-permeability reservoirs. Natural Gas Industry B, 4(4), 311-318.

[23] Liu, Y., Cheng, J., Zou, C., Lu, L., Jing, H., Ignition delay times of ethane under O2/CO2 atmosphere at different pressures by shock tube and simulation methods. Combustion and Flame. 2019 Jun 1; 204:380-90.

[24] Li, H., Haugen, G., Ditaranto, M., Berstad, D., and Jordal, K. (2011). Impacts of exhaust gas recirculation (EGR) on the natural gas combined cycle integrated with chemical absorption CO2 capture technology. Energy Procedia, 4, 1411-1418.

[25] Heywood, John B. Internal combustion engine fundamentals. McGraw-Hill 2nd edition., 2018. APA. Heywood, John B.